

Assessment of the Safety Factor Evolution of the Shotcrete Lining for Different Curing Ages

*Original*

Assessment of the Safety Factor Evolution of the Shotcrete Lining for Different Curing Ages / Oreste, P.; Spagnoli, G.; Luna Ramos, C. A.; Hedayat, A.. - In: GEOTECHNICAL AND GEOLOGICAL ENGINEERING. - ISSN 0960-3182. - STAMPA. - 37:6(2019), pp. 5555-5563. [10.1007/s10706-019-00990-2]

*Availability:*

This version is available at: 11583/2787828 since: 2020-01-31T12:46:13Z

*Publisher:*

Springer International Publishing

*Published*

DOI:10.1007/s10706-019-00990-2

*Terms of use:*

This article is made available under terms and conditions as specified in the corresponding bibliographic description in the repository

*Publisher copyright*

(Article begins on next page)

1 **Assessment of the safety factor evolution of the shotcrete lining for different curing**  
2 **ages**

3 Pierpaolo Oreste<sup>1</sup>, Giovanni Spagnoli<sup>2\*</sup>, Cesar Alejandro Luna Ramos<sup>3</sup>, Ahmadreza  
4 Hedayat<sup>4</sup>

5 <sup>1</sup> Full Professor, Department of Environmental, Land and Infrastructural Engineering,  
6 Politecnico di Torino, Corso Duca Degli Abruzzi 24, 10129 Torino, Italy,  
7 [pierpaolo.oreste@polito.it](mailto:pierpaolo.oreste@polito.it), ORCID: 0000-0001-8227-9807

8 <sup>2</sup> Global Project and Technology Manager Underground Construction, BASF Construction  
9 Solutions GmbH, Dr.-Albert-Frank-Straße 32, 83308 Trostberg, Germany, \*  
10 [giovanni.spagnoli@basf.com](mailto:giovanni.spagnoli@basf.com), ORCID: 0000-0002-1866-4345

11 <sup>3</sup> Professor, Faculty of Engineering, Universidad Mariana, Faculty of Engineering,  
12 Universidad Mariana, Calle 18 No. 34-104, Pasto, Colombia, [celuna@umariana.edu.co](mailto:celuna@umariana.edu.co).  
13 Former MSc student at Department of Environmental, Land and Infrastructural Engineering,  
14 Politecnico di Torino, Corso Duca Degli Abruzzi 24, 10129 Torino, Italy

15 <sup>4</sup> Assistant Professor, Department of Civil and Environmental Engineering, Colorado School  
16 of Mines, 1500 Illinois Street, Golden, CO 80401, USA, [hedayat@mines.edu](mailto:hedayat@mines.edu), ORCID: 0000-  
17 0002-7143-7272

18 **Abstract**

19 The behavior of the shotcrete linings during the tunnel construction is complex due to the  
20 variability of its mechanical characteristics during the curing time. During the curing time, the  
21 lining is loaded along with the excavation face of the tunnel advance. A new calculation  
22 procedure involving two analytical methods, i.e. the convergence-confinement method and  
23 hyperstatic reaction method have been developed. By means of these two methods, it is  
24 possible to assess the evolution of the stress state in the lining, and therefore, also of the  
25 safety factor with respect to the failure in compression of the shotcrete. Due to the analysis of

26 the safety factor evolution over time, it is possible to correctly design the lining, to choose the  
27 type of sprayed concrete and to define the maximum admissible advance rate of the  
28 excavation face, in order not to critically load the lining. In the following paper, after having  
29 shown the definition of the safety factor, a parametric analysis is performed, in order to  
30 investigate the evolution of the safety factor of the lining for two different rock types, three  
31 different shotcrete types and two tunnel advance rates have been considered.

32 **Key words:** sprayed concrete; convergence-confinement method; hyperstatic reaction  
33 method; accelerator; safety factor; curing age.

34 **No. of Figs: 5**

35

36 **Nomenclature**

37	$b$	Depth of the lining considered, equal to 1m in the two-dimensional problem
38		taken into consideration
39	$c_{rm}$ peak	Peak cohesion of the rock mass
40	$c_{rm}$ res	Residual cohesion of the rock mass
41	$E_{rm}$	Elastic modulus of the rock mass
42	$E_{SC}$	Elastic modulus of the sprayed concrete with varying time $t$ (in hours) after the
43		lining installation in the studied section
44	$E_{SC,\infty}$	Asymptotic values of the elastic modulus of the sprayed concrete reached for
45		high time values
46	FS	Safety factor
47	$M_{i,j}$	Bending moment in the $i$ -th node, at the load step $j$ -th
48	$N_{i,j}$	Normal force in the $i$ -th node, at the load step $j$ -th
49	$t$	Lining thickness
50	$\nu$	Poisson ratio
51	$\alpha$	Exponent of the exponential equation, which characterizes the curing rate, i.e.
52		the evolution of mechanical parameters (elastic modulus and uniaxial
53		compressive strength) of SC over time
54	$\phi_{rm}$ peak	Peak friction angle of the rock mass
55	$\phi_{rm}$ res	Residual friction angle of the rock mass
56	$\psi$	Dilatancy

57	$\sigma_{n,max,i,j}$	Maximum normal stress acting inside the sprayed concrete in correspondence
58		of a node
59	$\sigma_{SC}$	Unconfined compressive strength of the sprayed concrete with varying time t
60		(in hours) after the lining installation in the studied section
61	$\sigma_{SC,\infty}$	Asymptotic values of the Unconfined compressive strength of the sprayed
62		concrete, reached for high t values
63		

64 **Introduction**

65 DIN 18551 (2014) defines sprayed concrete (or shotcrete), abbreviated here as SC, as  
66 *“concrete which is conveyed under pressure through a pneumatic hose or pipe and projected*  
67 *into place at high velocity, with simultaneous compaction”* (see Fig. 1).



68

69 **Fig. 1 Sprayed concrete trials in a job site.**

70 Because SC takes care of stability problems in tunnels and other underground constructions  
71 (Melbye 1994) immediately after the installation, early-age strength and time-dependent  
72 behavior of SC both in soil and rock ground conditions is relevant (Thomas 2009);  
73 furthermore the time dependent behavior is frequently more important than its ultimate  
74 strength, because the advance rate (AR) of the tunnel face is strongly influenced by the rate  
75 of development of the SC early-age strength (Mohajerani et al. 2015). The time dependent  
76 behavior of shotcrete needs to be considered for realistic ground-support interactions and  
77 several constitutive models for shotcrete as a function of curing time currently exist in the

78 literature. Bryne (2014) conducted extensive compressive strength and Young's modulus  
79 evaluation of shotcrete with time and developed in-situ test techniques for determination of  
80 sprayed shotcrete bond strength. Several studies employed a constitutive law for time  
81 dependent stiffness and strength of the shotcrete (e.g., Pan and Huang, 1994; Graziani et al.  
82 2005; Schütz 2010).

83 The early-age strength of SC is frequently more important than its ultimate strength. The  
84 advance speed of tunnel operations is strongly influenced by the rate of development of  
85 early-age strength, since it determines, both in soft ground and weak rock, when excavation  
86 heading can proceed. As a matter of fact, re-entry is mainly driven by the tunnel drive  
87 progression to ensure the safety of personnel to continue development (Mohajerani et al.  
88 2015). Re-entry times range from 2 to 4 h, where the Unconfined Compressive Strength  
89 (UCS) reaches 1MPa (Clements 2004; Concrete Institute of Australia 2010), however, this  
90 value is not standardized and it can be also lower, if safety is ensured (see Rispin et al.  
91 2009). Iwaki et al. (2001) empirically determined that an UCS of 0.5–1MPa should be an  
92 adequate strength for SC to protect against rock-fall, although the safe re-entry times, based  
93 on strength measurements, is still determined on project basis (Mohajerani et al. 2015).

94 Therefore, additives are used to accelerate the hydration reaction (Thomas 2009).  
95 Accelerated SC has a shorter final setting time and higher early-age compressive strength  
96 compared with conventional concrete (Prudencio 1998) and it can be used in tunneling  
97 successfully. The use of accelerators allows for good adhesiveness, lower amount of  
98 rebounding, good spraying, and accelerated strength gain, as desired properties for  
99 shotcrete (Qiu et al. 2017).

100 Nowadays, accelerators for SC are normally based on combinations of aluminium salts  
101 (sulphates, hydroxides and hydroxysulphates) (DiNoia and Sandberg 2004). Aluminum  
102 sulfate is the most common type of accelerator being used (). In wet mix, the accelerator is  
103 added in liquid form at the nozzle during spraying. For dry mix, the accelerator can also be  
104 added as a fixed dosage in powder form when using pre-bagged mixes (Thomas 2009).

105 Accelerators considerably improve the setting which should be  $\leq 60$ min (prEN 934-5 2003)  
106 for SC applications, against the 6 to 7 h normally needed in Ordinary Portland Cement (De  
107 Belie et al. 2005).

108 In numerical modeling the curing of the cement in the SC lining is very important, as the  
109 mechanical improvements (compressive strength and elastic modulus) change the behavior  
110 of the linings. These transient conditions are a critical situation for the stability of the support  
111 structure during the tunnel construction, influencing the final equilibrium of the lining (Oreste  
112 2003).

113 There are several methods to numerically model sprayed concrete structures. Elastic method  
114 with a constant stiffness (e.g. Pöttler, 1990; Feenstra and de Borst 1993; Rokhar and  
115 Zachow, 1997), linear elastic material behavior models (for instance using the Hypothetical  
116 Modulus of Elasticity, HME) (e.g. Pöttler 1990), non-linear models considering strain  
117 hardening (e.g. Kotsovos and Newman 1978; Aydan et al. 1992; Moussa, 1993; Neville  
118 1995), elastic perfectly plastic constitutive models (e.g. Chen 1982; Hellmich et al. 1999;  
119 Thomas 2009), plastic models (e.g. Meschke 1996; Schütz et al. 2011; Schädlich and  
120 Schweiger 2014). Nuener et al. (2017) conducted a study and evaluated the influence of  
121 different constitutive models for shotcrete on the stresses and displacements in shotcrete  
122 shells in deep tunnels and reported different amount of creep and shrinkage in concrete.

123 The following paper considers the Converge Confinement Method (CCM) and the  
124 Hyperstatic Reaction Method (HRM) to jointly study in the detail the behavior of the tunnel  
125 support under external loads with different elastic modulus values of SC during the curing  
126 phase. The final stress state of the lining is the result of a complex loading mechanism due to  
127 the excavation face advance (while the SC hardens) and the corresponding variations in its  
128 mechanical characteristics (Oreste 2003). CCM generally requires a mean stiffness of the  
129 SC lining to obtain the support reaction line (Oreste 2003). In this research, the reaction line  
130 of the SC lining is considered as variable (curved and not linear), in order to simulate the  
131 curing effect of the SC during the loading phase of the lining. The variation over time of the

132 elastic modulus of SC is considered by modifying the stiffness of the support and therefore  
133 the slope of the reaction line of the SC lining. Time is indirectly considered by associating the  
134 different positions of the excavation face with respect to the studied section reached in the  
135 time, considering the evolution of the setting time of the SC and therefore to its elastic  
136 modulus.

137 CCM was useful to evaluate the magnitude of the various loading steps developing over time  
138 during the face excavation. In HRM method, the interaction between ground and support is  
139 represented by Winkler type springs. This method allows for determining the displacement of  
140 the lining and the developed bending moments and forces in order to design it (Oreste 2007;  
141 Do et al. 2014a). In the specific case, different loading steps obtained with the CCM, have  
142 been applied at the HRM model considering for each of these the effective stiffness value  
143 reached by the SC and hence by the support structure.

144 From the calculation results it is possible to determine the final mechanical conditions of the  
145 SC lining, that is, when the excavation face is far away from the tunnel section analyzed.  
146 Besides, it is also possible to determine, what occurs in the transition phases (for limited  
147 timings), when the applied load on the lining is not yet the final one. In this case the SC still  
148 has a strength and an elastic modulus lower than the final asymptotic values. From the  
149 comparison between the strength reached over the time of the SC and the final stress state  
150 in the lining, it is possible to evaluate the safety factor (FS) in the support structure. FS can  
151 be plotted as function of time after the installation of the lining in the evaluated section.  
152 These graphs are interesting as they allow to evaluate critical situations (minimum FS  
153 values) in the transition phases, when SC has not fully cured yet. In this research, after a  
154 brief description of the two methods employed for the calculation, a parametric analysis is  
155 conducted. The analysis considers three different SC types (with different curing ages) and  
156 two difference advancement rates (ARs) of the excavation face (with consequent different  
157 load stages of the lining). The analysis allows to assess the evolution of FS over time and to  
158 estimate critical phases during the transition load stages of the lining during the SC curing.

159 The combined analysis of the two calculation methods provided a detailed evaluation of the  
160 stress state of the support, which can consider both the effect of the mechanical  
161 characteristics of the employed SC (with the evolving curve of strength and stiffness with the  
162 time) and the advance rate of the excavation face.

### 163 **Analytical methods**

164 The analysis of the behavior of the SC linings, during the setting phase and, therefore, during  
165 the construction of the tunnel is quite complex with the traditional numerical methods. In fact,  
166 it is necessary to update the mechanical characteristics of the SC at each calculation step,  
167 linking them with the time after the installation of the lining in the investigated section and the  
168 position of the excavation face with respect to the studied section. The knowledge of the  
169 evolution of the mechanical parameters of the SC over time, in fact requires to define the  
170 elastic modulus of the SC at each calculation step. The position of the excavation face and,  
171 therefore, the progress of the excavation work, influences the loading mode of the lining in  
172 the studied section. In the three-dimensional numerical methods this happens automatically,  
173 since the construction of the tunnel is simulated according to the exact sequence of the  
174 excavation steps and the realization of the supports. In two-dimensional numerical methods,  
175 however, the position of the face is considered by inserting on the perimeter of the gallery an  
176 appropriate fictitious internal pressure, which is gradually decreasing as the excavation face  
177 advances.

178 Given the difficulties of the traditional numerical modeling to represent the correct evolution  
179 of the SC during the loading phase of the support, a new calculation procedure was  
180 developed (see Oreste et al. 2018a; 2018b) based on two analytical methods, very  
181 widespread in the field of tunnels and easy to use: the convergence-confinement method  
182 (CCM), see Oreste, (2009; 2014); Fahimifar and Hedayat (2008; 2010) and Spagnoli et al.  
183 (2016; 2017) and the hyperstatic reaction method (HRM), see Oreste (2007) and Do et al.  
184 (2014a; 2014b). The CCM allows to evaluate with a certain precision the various load steps  
185 acting on the lining, and, for each of them, to define the value of the elastic modulus reached

186 by the SC. This is done by determining the convergence-confinement curves of the tunnel  
187 and, subsequently, the reaction line of the lining in SC. The latter is determined by points,  
188 through the definition of different steps, based on the AR of the excavation face and the  
189 evolution of the elastic modulus of the SC over time.

190 The detailed analysis of the stress state in the lining is then assigned to the HRM. This  
191 analytical method uses a numerical solution to finite elements (FEM). The lining is simulated  
192 through a succession of one-dimensional elements (beam elements) connected in series  
193 through the nodes. On the same nodes of the numerical model, springs (normal and  
194 transversal) representing the interaction between the lining and the rock wall of the tunnel  
195 are connected. The load steps obtained from the analysis with the CCM are applied to the  
196 model and for each of them we proceed to update the elastic modulus of the SC in the one-  
197 dimensional elements. The results of the calculation for each load step allow to obtain the  
198 progress of the bending moments, of the normal forces and of the shear forces, as well as of  
199 the displacements, in the lining, along its whole length. At each load step, the results of that  
200 step are then added to the results achieved by all the previous loading steps.

201 If the bending moment  $M$  and the normal force  $N$  acting at each node of the lining (i) reached  
202 at the load step  $j$  are known, it is possible to determine the maximum normal stress  $\sigma_{n,max,i,j}$ ,  
203 acting inside the SC in correspondence of that node:

$$204 \quad \sigma_{n,max,i,j} = \frac{M_{i,j}}{\left(\frac{b \cdot s^2}{6}\right)} + \frac{N_{i,j}}{(b \cdot t)} \quad (1)$$

205 where:

206  $b$ : width of the lining considered, equal to 1m in the two-dimensional problem taken into  
207 consideration;

208  $M_{i,j}$ : bending moment in the  $i$ -th node, at the load step  $j$ -th;

209  $N_{i,j}$ : normal force in the  $i$ -th node, at the load step  $j$ -th;

210  $t$ : lining thickness.

211 Among all the values of  $\sigma_{n,max,i,j}$  obtained in the various nodes, the maximum value between  
212 the normal stress acting in the various nodes of the model is then identified, which is  
213 associated with the j-th load step:

$$214 \quad \sigma_{n,max,j} = \max(\sigma_{n,max,i,j}) \quad (2)$$

215 The local safety factor  $FS_j$  of the lining on the j-th load step is then evaluated according to the  
216 following equation:

$$217 \quad FS_j = \frac{\sigma_{c,j}}{\sigma_{n,max,j}} \quad (3)$$

218 where:

219  $\sigma_{c,j}$ : the strength reached by the SC at the j-th load step, knowing the time associated with  
220 each load step.

221 FS calculated above is a local FS, which allows to verify the possible presence of local failure  
222 over the SC lining. Local failures do not jeopardize the overall stability of the lining, however  
223 they can lead to cracks in the support which may turn out in a global failure. The design of  
224 the support must therefore consider local FS values to avoid global failures of the structure.

225 Since the time  $t$  following the realization of the lining in the studied section and the position of  
226 the excavation face (in particular the distance reached by the front with respect to the studied  
227 section) is associated with each loading step, the calculation procedure allows to plot FS of  
228 the SC lining depending on the time or on the distance reached by the excavation face with  
229 respect to the studied section. These trends make possible to quickly check whether there is  
230 a critical situation in the transient conditions of the lining, or if the minimum FS of the lining is  
231 reached in the long term (as an asymptotic value as discussed above). The procedure is able  
232 to compare the progress of FS for different types of SC (with and without accelerators) or  
233 also for different AR of the excavation face, so that the right type of SC can be chosen to  
234 ensure stability both during the construction of the work and in the long term, when the work  
235 has been completed.

## 236 **Results and discussion**

237 To analyze the evolution of FS of the SC lining with the calculation procedure developed, the  
 238 case of a circular tunnel with 7m radius excavated in two different rock types with RMR = 60  
 239 (fair), and RMR = 80 (good), as suggested by Bieniawski (1989), was analyzed. The  
 240 mechanical characteristics of the two rock masses considered are shown in Tables 1 and 2.

241 The lithostatic stress state of the rock mass  $p_0$  was assumed to be equal to 7MPa,  
 242 corresponding to a depth of the tunnel from the ground surface equal to about 300m.

Rock Mass Parameters	Units	Value
Elastic modulus ( $E_{rm}$ )	[MPa]	21,170
Poisson ratio ( $\nu$ )	[-]	0.30
Peak cohesion ( $c_{rm}$ peak)	[MPa]	1.50
Residual cohesion ( $c_{rm}$ res)	[MPa]	1.50
Peak friction angle ( $\phi_{rm}$ peak)	[°]	33
Residual friction angle ( $\phi_{rm}$ res)	[°]	33
Dilatancy ( $\psi$ )	[°]	16

243 **Table 1. Mechanical characteristics of the rocky type 1 (RMR = 60), considered in the**  
 244 **studied example.**

Rock Mass Parameters	Units	Value
Elastic modulus ( $E_{rm}$ )	[MPa]	57,500
Poisson ratio ( $\nu$ )	[-]	0.30
Peak cohesion ( $c_{rm}$ peak)	[MPa]	3.75
Residual cohesion ( $c_{rm}$ res)	[MPa]	3.75
Peak friction angle ( $\phi_{rm}$ peak)	[°]	42
Residual friction angle ( $\phi_{rm}$ res)	[°]	42
Dilatancy ( $\psi$ )	[°]	16

245 **Table 2. Mechanical characteristics of the rocky type 2 (RMR = 80), considered in the**  
 246 **studied example.**

247 Pöttler (1990) introduced the coefficient  $\alpha$  by suggesting a method to represent the variation  
 248 of the elastic modulus over the time.

$$E_{,t} = E_{,0} \cdot (1 - e^{-\alpha \cdot t}) \quad (4)$$

249 where:

- 250 •  $E_{,t}$  is the SC elastic modulus at the time  $t$ ;
- 251 •  $E_{,0}$  is the value of the asymptotic elastic modulus of the SC, for  $t = \infty$ ;

252 •  $\alpha$  is the exponent of the exponential equation, which characterizes the curing rate,  
253 i.e. the evolution of mechanical parameters over time (Oreste 2003).

254 The ratio between the elastic modulus and UCS is considered constant over time. This is given  
255 by the equation of Chang (1993):

$$\sigma_{c,t} = \left( \frac{E_{c,t}}{3.86} \right)^{1/0.6} \quad (5)$$

256 Where:

257  $\sigma_{c,t}$  is the UCS for the SC at the time  $t$ .

258 Three different SC types have been considered:

259 a) a SC with fast curing rate, (SC<sub>A</sub>) ( $\alpha=0.09$ );

260 b) a SC with medium curing rate, (SC<sub>B</sub>) ( $\alpha=0.05$ );

261 c) a SC with low curing rate, (SC<sub>C</sub>) ( $\alpha=0.03$ ).

262 For all three SC types, a final value of elastic modulus ( $E_{SC,\infty}=28\text{GPa}$ ) and unconfined  
263 compressive strength, UCS, ( $\sigma_{SC,\infty}= 27\text{MPa}$ ) was arbitrary assumed. The evolution over time  
264 of the elastic modulus and UCS was assumed to be identical, that means with the same  
265 value of  $\alpha$  (Weber 1979; Pöttler 1990; Oreste 2003):

$$266 \quad E_{SC} = E_{SC,\infty} \cdot (1 - e^{-\alpha t}) \quad (6)$$

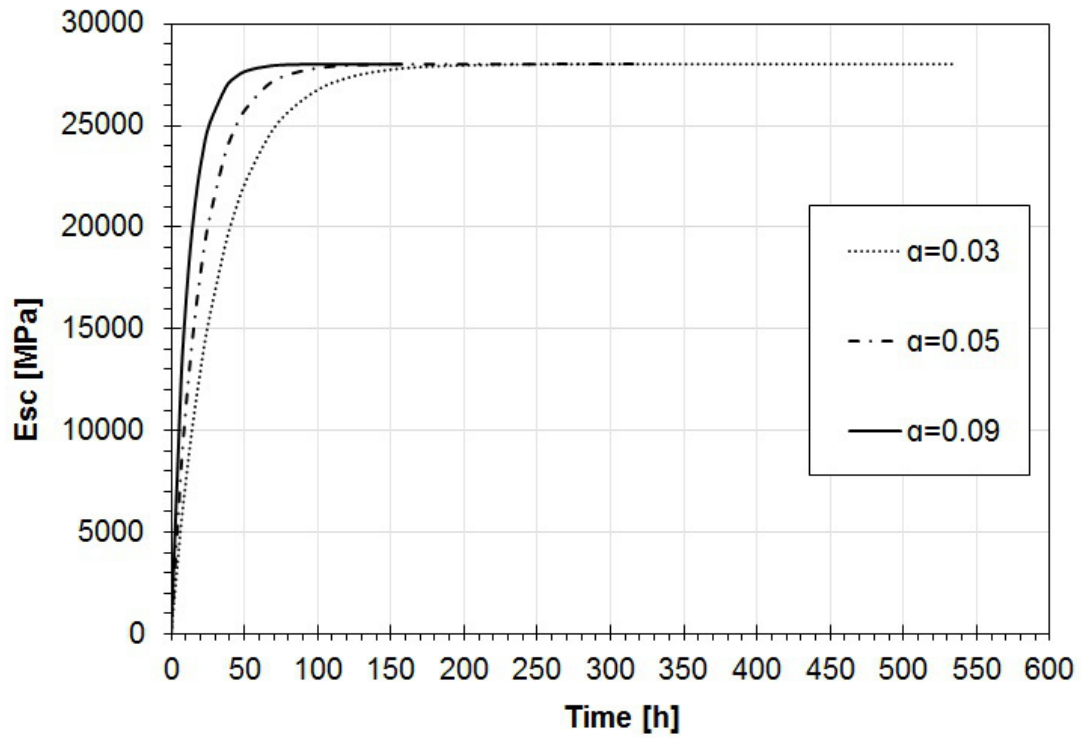
$$267 \quad \sigma_{SC} = \sigma_{SC,\infty} \cdot (1 - e^{-\alpha t}) \quad (7)$$

268 Where:

269  $E_{SC}$  and  $\sigma_{SC}$ : Elastic modulus and UCS of the SC with varying time  $t$  (in hours) after the lining  
270 installation in the studied section;

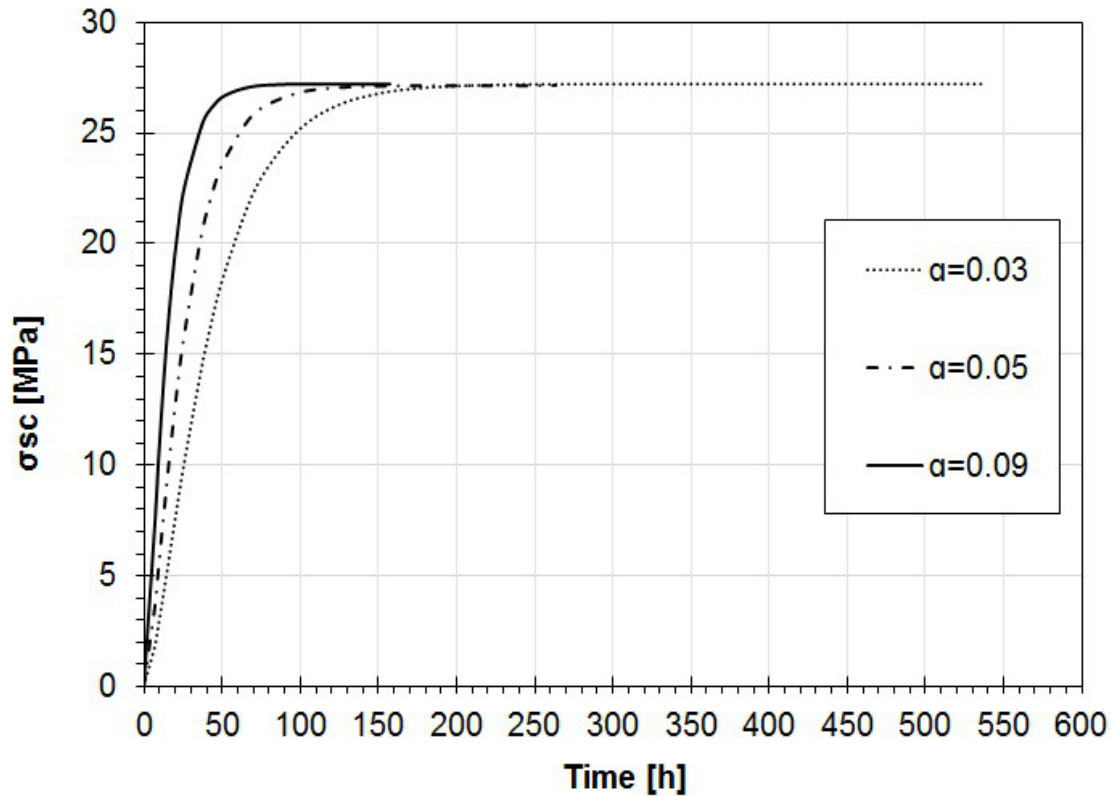
271  $E_{SC,\infty}$  and  $\sigma_{SC,\infty}$ : Asymptotic values of the elastic modulus and UCS of the SC, reached for  
272 high  $t$  values;

273 The trend over time of the elastic modulus and UCS of the SC for the three types considered  
274 is shown in Figures 2 and 3.



275

276 **Fig. 2 Trend of the elastic modulus over time for the three SC types considered in the**  
 277 **numerical example: SC<sub>A</sub>: SC with fast curing rate ( $\alpha=0.09$ ); SC<sub>B</sub>: SC with medium**  
 278 **curing rate ( $\alpha=0.05$ ) and SC<sub>C</sub>: SC with low curing rate ( $\alpha=0.03$ ).**

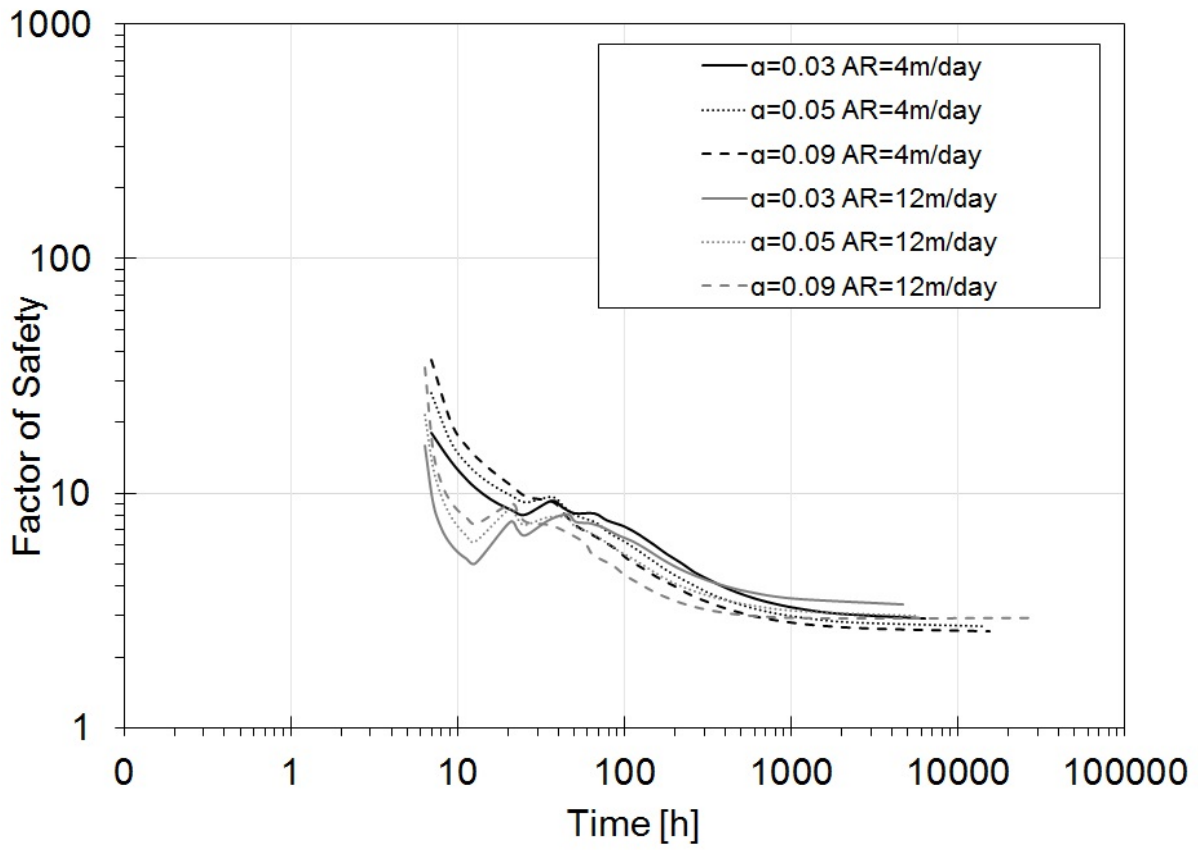


279

280 **Fig. 3 Trend of UCS over time for the three SC types considered in the numerical**  
 281 **example: SC<sub>A</sub>: SC with fast curing rate ( $\alpha=0.09$ ); SC<sub>B</sub>: SC with medium curing rate**  
 282 **( $\alpha=0.05$ ) and SC<sub>C</sub>: SC with low curing rate ( $\alpha=0.03$ ).**

283 Furthermore, two different ARs of the excavation face have been arbitrary considered:  
 284 4m/day and 12m/day. The two different rates produce different speed of the load application  
 285 to the lining, with consequences on the stress state induced in the SC.

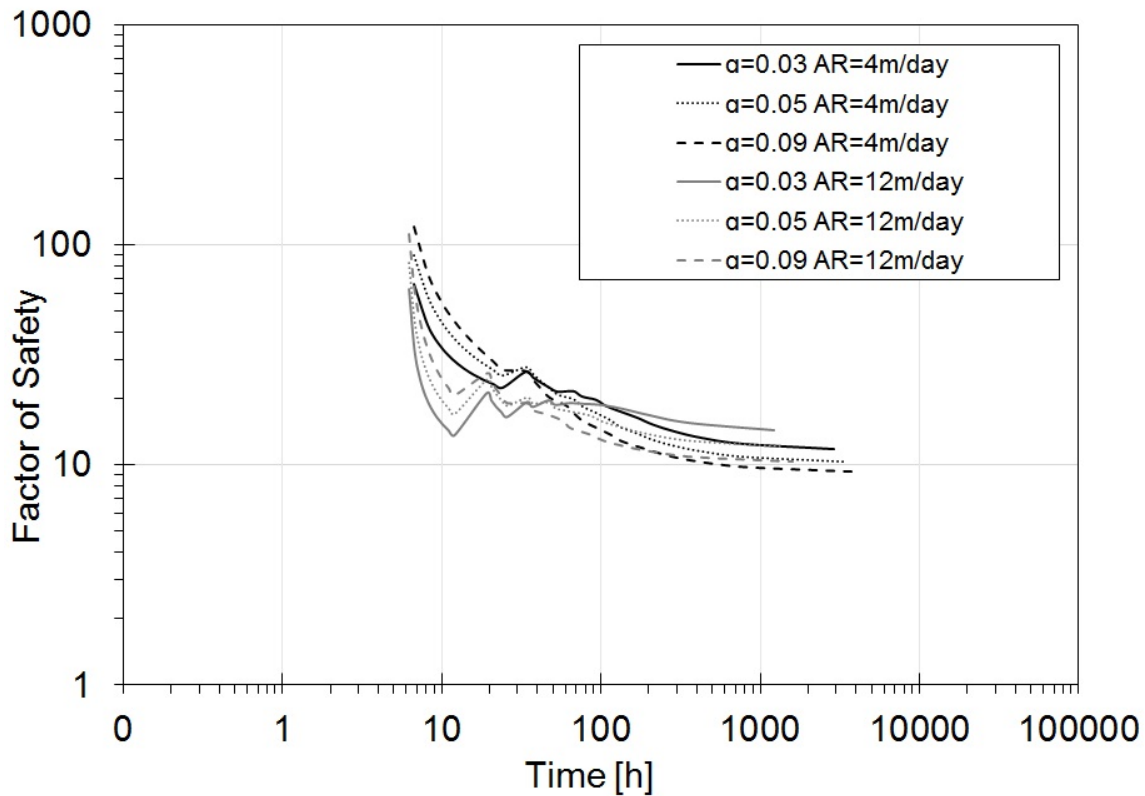
286 The calculation by first the CCM and then with the HRM allowed to determine the values of  
 287 the bending moments M and of the normal forces N along the development of the entire  
 288 lining. From the values of M and N the maximum normal stresses in the SC were obtained  
 289 for each load step and, then, FS with respect to the compression failure. Below the results in  
 290 terms of FS for the two rock masses, the three types of SC and the two ARs studied are  
 291 shown. FS are diagrammed according to the time following the lining installation in the  
 292 studied section.



293

294 **Fig. 4 Rock type 1: Evaluation of FS over time for the three SC types ( $SC_A$  ( $\alpha=0.09$ ),  $SC_B$**

295 **( $\alpha=0.05$ ) and  $SC_c$  ( $\alpha=0.03$ )) and two advance rates.**



296

297 **Fig. 5 Rock type 2: Evaluation of FS over time for the three SC types ( $SC_A$  ( $\alpha=0.09$ ),  $SC_B$**   
 298 **( $\alpha=0.05$ ) and  $SC_c$  ( $\alpha=0.03$ )) and two advance rates.**

299 The analysis of the results shows above all that the same SC lining has lower **local** FS for  
 300 the rock type 1, the poorest one among the two considered (Fig. 4). In addition, we note the  
 301 influence of the type of SC and the AR on FS in both rock masses, mainly for the rock mass  
 302 with higher geomechanical quality (type 2), see Fig. 5. In general, the long-term FS is lower  
 303 for fast-curing SCs and lower ARs. AR results to have a negligible effect in the poorest rock  
 304 mass.

305 In the transitory conditions, however, there is the presence of relative minima, which may be  
 306 significant, above all for high ARs and slow curing rate. This phenomenon is more  
 307 pronounced in the rock mass of superior geomechanical quality. Among the 12 cases  
 308 studied, just for the case of rock masses type 2,  $v = 12\text{m/day}$  and type  $SC_c$  (with  $\alpha$  coefficient  
 309 of 0.03) a minimum value of FS in the transient condition is noticed (after a few hours

310 compared to the lining installation) lower than the final asymptotic value, representative of  
311 the long-term condition.

312 This circumstance is particularly significant and requires a lot of attention by the tunnel  
313 engineers. It can indicate the presence of critical aspects regarding the stability of the lining  
314 in a transitory condition, when the SC has not yet completed the curing phase during the  
315 tunnel construction.

## 316 **Conclusions**

317 A new calculation procedure has been used which is able to study in detail the mechanical  
318 behavior of the lining during the tunnel construction. This procedure is based on two  
319 analytical methods used in succession: the convergence-confinement method (CCM) and the  
320 hyperstatic reaction method (HRM). The first one allows evaluating the load steps applied to  
321 the lining and, for each one, the value of the elastic modulus reached by the SC. The second  
322 helps to calculate the progression of moments, internal forces and displacements, from the  
323 results obtained from the first. From the bending moment and the axial force values, it is then  
324 possible to determine the safety factor along the perimeter of the lining and the minimum  
325 value of the safety factor, representative for the entire support. This safety factor is then  
326 plotted over time in order to evaluate the stability conditions of the lining during the tunnel  
327 construction.

328 Subsequently, a parametric analysis was presented analyzing the behavior of the support in  
329 two different types of rock mass types, considering two ARs of the excavation face and three  
330 types of SC, with different curing rates. The study revealed that, generally, the minimum  
331 safety factor is reached in the long term, when the curing of the SC is completed. However,  
332 there are circumstances that produce a minimum of the safety factor in the transitory  
333 conditions, after a few hours from the lining installation. In these circumstances, the major  
334 problems with the stability of the lining are in the short term, rather than in the long term. This

335 can happen above all in the medium-high geomechanical rock types, in the presence of SC  
336 with relatively slow curing, with high ARs.

### 337 **References**

- 338 1. Aydan, O., Sezaki M. and Kawamoto T. (1992). "Mechanical and numerical modelling  
339 of shotcrete," in Pande, G., Pietruszczack, S. (Eds.), Numerical Models in  
340 Geomechanics, Taylor and Francis, London, pp. 707-7016.
- 341 2. Bieniawski, Z. T. (1978). "Determining rock mass deformability". Int. J. Rock Mech.  
342 Min.Sci., 15, 335–343.
- 343 3. Bryne, L. E. (2014). "Time Dependent Material Properties of Shotcrete for Hard Rock  
344 Tunneling." Ph.D Thesis, Stockholm, Sweden.
- 345 4. Clements, M. (2004). "Comparison of methods for early age strength testing of  
346 sprayed fibre reinforced concrete." In: Bernard, E.S. (Ed.), Proceedings of the 2nd  
347 International Conference on Engineering Developments in Sprayed Fibre Reinforced  
348 Concrete, Cairns, Queensland, Australia. Taylor and Francis Group, London, pp. 81–  
349 87.
- 350 5. Chen, W.F. (1982). Plasticity in Reinforced Concrete. McGraw-Hill, New York.
- 351 6. Chang, Y., and Stille, H. (1993). "Influence of early age properties of shotcrete on  
352 tunnel construction sequences." in Wood, D.F., Morgan, D.R. (Eds.), Shotcrete for  
353 Underground Support VI, American Society of Civil Engineers, Reston, pp. 110-117.
- 354 7. Chang, Y. (1994). "Tunnel support with shotcrete in weak rock- A rock mechanics  
355 study." Ph.D. Thesis, Division of Soil and Rock Mechanics, Royal Institute of  
356 Technology, Stockholm, Sweden.
- 357 8. Concrete Institute of Australia (2010). Shotcrete in Australia. Concrete Institute of  
358 Australia, Rhodes, Australia.
- 359 9. De Belie, N., Grosse, C.U., Kurz, J., and Reinhardt, H.W. (2005). "Ultrasound  
360 monitoring of the influence of different accelerating admixtures and cement types for

- 361 shotcrete on setting and hardening behavior.” *Cement Concrete Res.*, 35, 2087 –  
362 2094.
- 363 10. DIN (2014). *Spritzbeton - Nationale Anwendungsregeln zur Reihe DIN EN 14487 und*  
364 *Regeln für die Bemessung von Spritzbetonkonstruktionen*, Beuth Verlag GmbH,  
365 Berlin (in German).
- 366 11. DiNoia, T.P., and Sandberg, P.J. (2004). Alkali-free shotcrete accelerator interactions  
367 with cement and admixtures. 2<sup>nd</sup> International Conference on Engineering  
368 Developments in Shotcrete, pp. 137-144, A.A. Balkema Publishers, Leiden, London.
- 369 12. Do, N.A., Dias, D., Oreste, P., and Djeran-Maigre, I. (2014a). “A new numerical  
370 approach to the hyperstatic reaction method for segmental tunnel linings.” *Int. J.*  
371 *Numer. Anal. Meth. Geomech.*, 38, 1617–1632.
- 372 13. Do, N.A., Dias, D., Oreste, P., and Djeran-Maigre, I., (2014b). “The behavior of the  
373 segmental tunnel lining studied by the hyperstatic reaction method.” *Eur. J.*  
374 *Environmental Civil Eng.* 18(4), 489–510.
- 375 14. Fahimifar, A. and Hedayat, A. (2008). “Determination of ground response curve of the  
376 supported tunnel considering progressive hardening of shotcrete lining.” *Proceedings*  
377 *of the 5th Asian Rock Mechanics Symposium*, Tehran, Iran, November 24-26.
- 378 15. Fahimifar, A. and Hedayat, A. (2010). “Elasto-plastic analysis in conventional  
379 tunnelling excavation.” *Proc. Inst. Civ. Eng. Geotech. Eng.*, 163(1), 37-45, doi:  
380 10.1680/geng.2010.163.1.37.
- 381 16. Feenstra, P.H., and de Borst, B. (1993). “Aspects of robust computational models for  
382 plain and reinforced concrete,” *Heron* 48(4), 5-73.
- 383 17. Graziani, A., Boldini, D., and Ribacchi, R. (2005). “Practical estimate of deformations  
384 and stress relief factors for deep tunnels supported by shotcrete.” *Rock Mech. Rock*  
385 *Engng.* 38 (5), 345–372.
- 386 18. Hellmich, C., Ulm, F.J. and Mang, H.A. (1999). „Multisurface chemoplasticity II:  
387 numerical studies on NATM-tunneling.” *J Eng. Mech.-ASCE*, 125(6): 702-714.

- 388 19. Iwaki, K., Hirama, A., Mitani, K., Kaise, S., Nakagawa, K. (2001). „A quality control  
389 method for shotcrete strength by pneumatic pin penetration test.” NDT and E  
390 International, 34(6), 395-402.
- 391 20. Kotsovos, M.D. and Newman, J.B. (1978). “Generalized stress-strain relation for  
392 concrete,” J. Eng. Mech.-ASCE,104: 845-856.
- 393 21. Melbye, T. (1994). Sprayed Concrete for Rock Support. MBT International  
394 Underground Construction Group, Zürich.
- 395 22. Meschke, G. (1996). “Elasto-viskoplastische Stoffmodelle für numerische  
396 Simulationen mittels der Methode der Finiten Elemente,” Habilitationsschrift, TU  
397 Wien.
- 398 23. Mohajerani, A., Rodrigues, D., Ricciuti, C., and Wilson, C. (2015). Early-Age Strength  
399 Measurement of Shotcrete. Journal of Materials, ID 470160,  
400 <http://dx.doi.org/10.1155/2015/470160>.
- 401 24. Moussa, A.M. (1993). Finite element modelling of shotcrete in tunnelling. PhD thesis,  
402 University of Innsbruck, Austria.
- 403 25. Neuner, M., Schreter, M., Unteregger, D., and Hofstetter, G. (2017). “Influence of the  
404 Constitutive Model for Shotcrete on the Predicted Structural Behavior of the Shotcrete  
405 Shell of a Deep Tunnel.” Materials, 10, 577, doi:10.3390/ma10060577.
- 406 26. Neville, A.M., Dilger, W.H., and Brooks, J.J. (1983). Creep of Plain and Structural  
407 Concrete. Construction Press, Harlow.
- 408 27. Oreste, P. (2003). “Procedure for Determining the Reaction Curve of Shotcrete Lining  
409 Considering Transient Conditions.” Rock Mech. Rock Eng., 36(3), 209–236, DOI  
410 10.1007/s00603-002-0043-z.
- 411 28. Oreste, P. (2007). “A numerical approach to the hyperstatic reaction method for the  
412 dimensioning of tunnel supports.” Tunn. Undergr. Sp. Tech., 22:185–205.
- 413 29. Oreste P. (2009). “The Convergence-Confinement Method: Roles and limits in  
414 modern geomechanical tunnel design.” American Journal of Applied Sciences 6(4),  
415 757-771.

- 416 30. Oreste P. (2014). "The Determination of the tunnel structure loads through the  
417 analysis of the Interaction between the void and the support using the convergence-  
418 confinement method." *F American Journal of Applied Sciences*, 11(11), 1945-1954.
- 419 31. Oreste, P., Spagnoli, G., Luna Ramos, C.A., and Seville, L. (2018). "The Hyperstatic  
420 Reaction Method for the Analysis of the Sprayed Concrete Linings Behavior in  
421 Tunneling." *Geotech. Geol. Eng.*, <https://doi.org/10.1007/s10706-018-0454-6>.
- 422 32. Oreste, P., Spagnoli, G., and Luna Ramos, C.A., (2018b). "The Elastic Modulus  
423 Variation During the Shotcrete Curing Jointly Investigated by the Convergence-  
424 Confinement and the Hyperstatic Reaction Methods." *Geotech. Geol. Eng.*,  
425 <https://doi.org/10.1007/s10706-018-0698-1>.
- 426 33. Pan, Y.W., and Huang, Z.L. (1994). "A model for the time dependent interaction  
427 between rock and shotcrete support in a tunnel." *Int. J. Rock Mech. Min. Sci.* 31(3),  
428 213-219.
- 429 34. Pöttler, R. (1990). "Time-dependent rock—Shotcrete interaction a numerical  
430 shortcut." *Comp. Geotech.*, 9(3), 149-169.
- 431 35. prEN 934-5 (2003) *Admixtures for Concrete, Mortar and Grout—Part 5: Admixtures*  
432 *for Sprayed Concrete—Definitions, Requirements and Conformity*.
- 433 36. Prudencio, L.R. Jr (1998). "Accelerating admixture for shotcrete." *Cem. Concr.*  
434 *Compos.*, 20, 213–219.
- 435 37. Qiu, Y., Ding, B., Gan, J., Guo, Z., Zheng, C., Jiang, H. (2017). "Mechanism and  
436 preparation of liquid alkali-free liquid setting accelerator for shotcrete". *IOP Conf. Ser.*  
437 *Mater. Sci. Eng.*, 182, 012034, doi:10.1088/1757-899X/182/1/012034.
- 438 38. Rispin, M., Howard, D., Kleven, O. B., Garshol, K., Gelson, J. (2009). "Safer, Deeper,  
439 Faster: Sprayed Concrete—An Integral Component of Development Mining,"  
440 *Australian Centre for Geomechanics*.
- 441 39. Rokhar, R.B., and Zachow, R. (1997). "Ein neues Verfahren zur taglichen Kontrolle  
442 der Auslastung einer Spritzbetonschale," *Felsbau* 15(6), 430-434.

- 443 40. Schädlich, B. and Schweiger, H.F. (2014). "A new constitutive model for shotcrete,"  
444 in: Hicks, M.A., Brinkgreve, R.B.J., Rohe, A. (Eds.), Numerical Methods in  
445 Geotechnical Engineering. Taylor & Francis, Oxam, pp. 103-108.
- 446 41. Schütz, R. (2010). "Numerical modelling of shotcrete for tunneling" Ph.D Thesis,  
447 Imperial College London, UK.
- 448 42. Schütz, R., Potts, D.M., and Zdravkovic, L. (2011). "Advanced constitutive modelling  
449 of shotcrete: Model formulation and calibration." *Comput. Geotech.* 38(6):834–845.
- 450 43. Spagnoli, G., Oreste, P., and Lo Bianco, L. (2016). "New Equations for Estimating  
451 Radial Loads on Deep Shaft Linings in Weak Rocks." *Int. J. Geomech.*, 16(6),  
452 06016006, [https://doi.org/10.1061/\(ASCE\)GM.1943-5622.0000657](https://doi.org/10.1061/(ASCE)GM.1943-5622.0000657).
- 453 44. Spagnoli, G., Oreste, P., and Lo Bianco, L. (2017). "Estimation of Shaft Radial  
454 Displacement beyond the Excavation Bottom before Installation of Permanent Lining  
455 in Nondilatant Weak Rocks with a Novel Formulation." *Int. J. Geomech.*, 17(9),  
456 04017051 [https://doi.org/10.1061/\(ASCE\)GM.1943-5622.0000949](https://doi.org/10.1061/(ASCE)GM.1943-5622.0000949).
- 457 45. Thomas, A. (2009) *Sprayed concrete lined tunnels*. Taylor & Francis, Oxon.
- 458 46. Weber, J. W. (1979). "Empirische Formeln zur Beschreibung der  
459 Festigkeitsentwicklung und der Entwicklung des E-moduls von Beton." *Betonwerk-*  
460 *und-Fertigteilechnik*, 753–759.
- 461

462 **Figure caption**

463 **Fig. 1 Sprayed concrete trials in a job site.**

464 **Fig. 2 Trend of the elastic modulus over time for the three SC types considered in the**  
465 **numerical example: SC<sub>A</sub>: SC with fast curing rate ( $\alpha=0.09$ ); SC<sub>B</sub>: SC with medium**  
466 **curing rate ( $\alpha=0.05$ ) and SC<sub>C</sub>: SC with low curing rate ( $\alpha=0.03$ ).**

467 **Fig. 3 Trend of UCS over time for the three SC types considered in the numerical**  
468 **example: SC<sub>A</sub>: SC with fast curing rate ( $\alpha=0.09$ ); SC<sub>B</sub>: SC with medium curing rate**  
469 **( $\alpha=0.05$ ) and SC<sub>C</sub>: SC with low curing rate ( $\alpha=0.03$ ).**

470 **Fig. 4 Rock type 1: Evaluation of FS over time for the three SC types (SC<sub>A</sub> ( $\alpha=0.09$ ), SC<sub>B</sub>**  
471 **( $\alpha=0.05$ ) and SC<sub>C</sub> ( $\alpha=0.03$ )) and two advance rates.**

472 **Fig. 5 Rock type 2: Evaluation of FS over time for the three SC types (SC<sub>A</sub> ( $\alpha=0.09$ ), SC<sub>B</sub>**  
473 **( $\alpha=0.05$ ) and SC<sub>C</sub> ( $\alpha=0.03$ )) and two advance rates.**

474

475 **Table caption**

476 **Table 1. Mechanical characteristics of the rock type 1 (RMR = 60), considered in the**  
477 **studied example.**

478 **Table 2. Mechanical characteristics of the rock type 2 (RMR = 80), considered in the**  
479 **studied example.**